Since January 2020 Elsevier has created a COVID-19 resource centre with free information in English and Mandarin on the novel coronavirus COVID-19. The COVID-19 resource centre is hosted on Elsevier Connect, the company's public news and information website.

Bioorg. Med. Chem. Lett. 43 (2021) 128099

Contents lists available at ScienceDirect

Bioorganic & Medicinal Chemistry Letters

journal homepage: www.elsevier.com/locate/bmcl

Promising anti-SARS-CoV-2 drugs by effective dual targeting against the viral and host proteases

Samia A. Elseginy [a,e], Bahgat Fayed [b,f], Rania Hamdy [b,g], Noura Mahrous [c], Ahmed Mostafa [c], Ahmed M. Almehdi [d], Sameh S. M. Soliman [b,h,*]

[a] Molecular Modelling Lab, Biochemistry School, Bristol University, Bristol, UK
[b] Research Institute for Medical and Health Sciences, University of Sharjah, P.O. Box 27272, Sharjah, United Arab Emirates
[c] Centre of Scientific Excellence for Influenza Viruses, National Research Centre, Giza 12622, Egypt
[d] College of Sciences, University of Sharjah, P.O. Box 27272, Sharjah, United Arab Emirates
[e] Green Chemistry Department, Chemical Industries Research Division, National Research Centre, P.O. Box 12622, Egypt
[f] Chemistry of Natural and Microbial Product Department, National Research Centre, Cairo 12622, Egypt
[g] Faculty of Pharmacy, Zagazig University, Zagazig 44519, Egypt
[h] College of Pharmacy, University of Sharjah, P.O. Box 27272, Sharjah, United Arab Emirates

ARTICLE INFO

Keywords:
SARS-CoV-2
COVID-19
Dual antiviral activity
Anti-M^{pro}
Anti-PLpro
Anti-furin

ABSTRACT

SARS-CoV-2 caused dramatic health, social and economic threats to the globe. With this threat, the expectation of future outbreak, and the shortage of anti-viral drugs, scientists were challenged to develop novel antivirals. The objective of this study is to develop novel anti-SARS-CoV-2 compounds with dual activity by targeting valuable less-mutated enzymes. Here, we have mapped the binding affinity of >500,000 compounds for potential activity against SARS-CoV-2 main protease (M^{pro}), papain protease (PLpro) and human furin protease. The enzyme inhibition activity of most promising hits was screened and tested in vitro on SARS-CoV-2 clinical isolate incubated with Vero cells. Computational modelling and toxicity of the compounds were validated. The results revealed that 16 compounds showed potential binding activity against M^{pro}, two of them showed binding affinity against PLpro and furin protease. Respectively, compounds **7** and **13** showed inhibition activity against M^{pro} at IC_{50} 0.45 and 0.11 μM, against PLpro at IC_{50} 0.085 and 0.063 μM, and against furin protease at IC_{50} 0.29 μM. Computational modelling validated the binding affinity against all proteases. Compounds **7** and **13** showed significant inhibition activity against the virus at IC_{50} 0.77 and 0.11 μM, respectively. Both compounds showed no toxicity on mammalian cells. The data obtained indicated that compounds **7** and **13** exhibited potent dual inhibition activity against SARS-CoV-2. The dual activity of both compounds can be of great promise not only during the current pandemic but also for future outbreaks since the compounds' targets are of limited mutation and critical importance to the viral infection.

Coronavirus pandemic disease 2019 (COVID-19) is an emerging public health problem that is caused by severe acute respiratory syndrome coronavirus 2 (SARS-CoV-2).[1] In regards, several antiviral drugs have been proposed including those targeting the viral and/or host proteins,[2] neutralizing antibodies that target SARS-CoV-2,[3] repurposing of other antiviral drugs.[4] Further, some marketed drugs including hydroxychloquine, lopinavir, chloroquine and remdesivir were evaluated.[5–7] However, the infection continues to be extremely challenging, and the cases sill increasing and no treatment was effective.[8] Therefore, there is an urgent need for the design and development of novel small molecules with promising anti-SARS-CoV-2 activity.

SARS-CoV-2 requires two critical proteases, the main protease (M^{pro}) and papain-like protease (PLpro) to complete its life cycle.[9] Both proteases are essential for SARS-CoV-2 replication,[10] which renders them as important targets for the development of anti-SARS-CoV-2 drugs. On the other hand, viral entry requires the cleavage of spike glycoprotein at 682–689 residues,[11] which is performed by human furin protease.[12] It enhances the viral fusion to the host cell.[13] This process is characteristic to SARS-CoV-2 when compared to other coronaviruses.[12] Furin protease belongs to proprotein/ prohormone convertases (PCs) family that is ubiquitously expressed in human.[14] This makes human furin protease as an important target, particularly to overcome future evolved resistance

* Corresponding author at: Department of Medicinal Chemistry, College of Pharmacy, University of Sharjah, Sharjah 27272, United Arab Emirates.
E-mail address: ssoliman@sharjah.ac.ae (S. S. M. Soliman).

https://doi.org/10.1016/j.bmcl.2021.128099
Received 17 February 2021; Received in revised form 25 April 2021; Accepted 5 May 2021
Available online 10 May 2021

Table 1
Compound supplier ID and their binding energies against M^{pro}, PLpro viral proteases and human furin protease.

No	Compound supplier ID	M^{pro}	PLpro	Furin
	Native ligand*	−10.35	−11.63	−17.03
1	MCULE-5559121280–0	−11.24	−12.13	−10.85
2	Molport-002–542-400	−11.14	−13.65	−11.58
3	MCULE-8748749803–0	−12.55	−15.88	−12.79
4	Molport-004–271-700	−10.63	−13.72	−11.35
5	MCULE-4469963687–0	−10.4	−12.9	−11.34
6	Molport-007–594-574	−11.42	−13.39	−10.97
7	MCULE-3732245601–0	−13.7	−16.02	−13.43
8	Molport-004–251-833	−11.34	−13.02	−10.77
9	MCULE-3135581181–0	−11.17	−15	−12.21
10	Moloport-005–550-475	−10.4	−12.39	−10.32
11	MCULE-4485704859–0	−11.33	−13.62	−12.06
12	MolPort-005–115-349	−11.32	−14.79	−11.92
13	MCULE-7013373725–0	−11.15	−13.62	−13.41
14	MCULE-4934649484–0	−10.5	−13.32	−10.89
15	MCULE-2167531027–0	−17.98	−17.46	−13.83
16	MCULE-3570302261–0	−13.67	−12.09	−11.19

* Native ligand of M^{pro}; *tert*-Butyl (1-((S)-1-(((S)-4-(benzylamino)-3,4-dioxo-1-((S)-2-oxopyrrolidin-3-yl) butan-2-yl) amino)-3-cyclopropyl-1-oxopropan-2-yl)-2-oxo-1,2-dihydropyridin-3-yl) carbamate (alpha-ketoamide 13b), Native ligand of PLpro; GRL0617, Native ligand of furin; Co-crystalized peptide.

by the virus.

A very efficient strategy to fight against SARS-CoV-2 is to develop an inhibitor with dual activities. For this purpose, a pharmacophore-based virtual screening against M^{pro}, PLpro and furin was applied. The process depended on (i) screening a library of compounds against 3D pharmacophore that is build up on the interactions of peptidomimetic N3 (peptide-like irreversible inhibitors – Michael acceptor)[1] or α-ketoamide 13b [*tert*-butyl (1-((S)-1-(((S)-4-(benzylamino)-3,4-dioxo-1-((S)-2-oxopyrrolidin-3-yl) butan-2-yl) amino)-3-cyclopropyl-1-oxopropan-2-yl)-2-oxo-1,2-dihydropyridin-3-yl) carbamate][15] inhibitors with M^{pro}, (ii) molecular docking against the three enzymes followed by ranking the binding scores of the molecules, and (iii) the molecules showing good binding score against at least two proteases were selected for further biological activity.

Virtual screening was run against both viral proteases M^{pro} and PLpro and human furin protease. Initially, 500,000 compounds available in the MCULE and MolPort commercial databases were screened against M^{pro} enzyme. M^{pro} was used first to construct a 3D pharmacophore, because the enzyme operates at no<11 cleavage sites on the large polyprotein,[15] while there is no human proteases have a similar cleavage specificity. This makes the selected molecules obtained from this filtration step are unlikely toxic. Around 1350 compounds were selected based on 7 pharmacophore features of M^{pro}. This was followed by molecular docking against the binding pockets of M^{pro}, PLpro and furin. Around 100 compounds (Suppl. Table 1) with comparable binding energy to the native ligands were selected and visually re-screened. Only 16 compounds showing the best scoring and binding affinity (Tables 1 and Fig. 1) were selected for further biological activity. Virtual screening procedure was summarized in Fig. 2.

Analysis of substrate binding site of SARS-CoV-2 M^{pro} was carried out to build a 3D structure-based pharmacophore. The newly released crystal structure of SARS-CoV-2 M^{pro} (PDB: 6LU7, www.rcsb.org), where N3 is covalently-bonded, and the second co-crystal structure (PDB: 6Y2G, www.rcsb.org), where 13b interacted with SARS-CoV-2 M^{pro}, provide a solid basis to understand the key residues necessary for the enzyme interactions. N3 and 13b inhibit SARS-CoV (2003) M^{pro} by exhibiting a two-step irreversible covalent binding mechanism[16]. M^{pro} is a dimer composed of three domains, domain I (residues 8–101), domain II (residues 102–184) and domain III (residues 201–303). Domains II and III are connected by a loop region (residues 185–200), and the substrate-binding site is in a cleft between domain I and domain II.

The binding of N3 with M^{pro} was analysed and showed that N3 formed H-bond with Glu144, His163, His164, Gln189, and Thr190, covalent bond with Cys145 and hydrophobic interactions with His41, Met49, Phe140, Leu141, Met165, Leu167, Pro168, and Ala191. The residues that were involved in the interaction of N3 were the same as for 13b molecule.[17] However, compound 13b formed additional H-bonds with His41, Cys145 and Glu166, while maintaining the same hydrophobic interactions. A 3D pharmacophore was built using PLIF protocol in MOE software based on the interactions of N3 and 13b compounds with M^{pro} (PDB: 6LU7 and 6Y2G, respectively). The developed pharmacophore (Fig. 3) consisted of seven features including two H-bond donor centres, three H-bond acceptor centres, one hydrogen bond donor/ acceptor and a hydrophobic centre. Subsequently, 500,000 molecules obtained from MCULE and MolPort libraries were screened against the 3D pharmacophore. A total of 1,350 molecules that match at least 5 of the 7 features were selected.

The substrate binding pockets of PLpro and furin proteases were studied. The PLpro (PDB: 7JRN, www.rcsb.org) active site was made of Asp165, Glu168, Leu163, Gly164, Pro248, Pro249, Tyr265, Tyr269 Glu270, Tyr274, and Thr302, while the catalytic or substrate binding pocket of furin (PDB: 6HLB, www.rcsb.org) was formed of key residues including Arg188, Met189, Asp191, Asn192, Arg193, Glu229, Val231, Asp233, Asp259, Lys261, Arg298, and Trp328[12–13]. These residues interacted with the viral spike protein cleavage site. The co-crystallized peptide ligand formed H-bonds with Asp154, Asn192, Ser253 and Asp306. The retained molecules were docked against the three enzymes M^{pro}, PLpro and furin. The co-crystal (BDP: 6Y2G) bonded to 13b was used to dock the molecules against M^{pro}. On the other hand, the molecular docking against PLpro and furin was performed on the crystal structures (PDB: 7JRN) and (PDB: 6HLB), respectively.

The binding scores due to the re-docking of the co-crystallized ligands with M^{pro}, PLpro and furin proteases were −10.35, −11.63 and −17.03 kcal/mol, respectively (Table 1). The binding scores of M^{pro} and PLpro were used as a cut-off for selecting the promising hits. Since there are no compounds showed binding score better than the native ligand of furin complex, the top 200 molecules with the highest binding score were selected . A total of 100 compounds were then selected based on the lowest binding score against at least two protease enzymes (Suppl. Table 1). A final short list of 16 compounds was selected based on visual inspection with the following selection criteria: (i) molecules that have scaffold diversity, (ii) molecules showing good binding mode within the binding pocket of the three enzymes, and (iii) molecules containing at least one hydrogen bond acceptor or donor pharmacophore. The shortlisted compounds (Tables 1 and Fig. 1) were screened for pan assay interference (PAINS) using the online PAINS filters. The Hit compounds

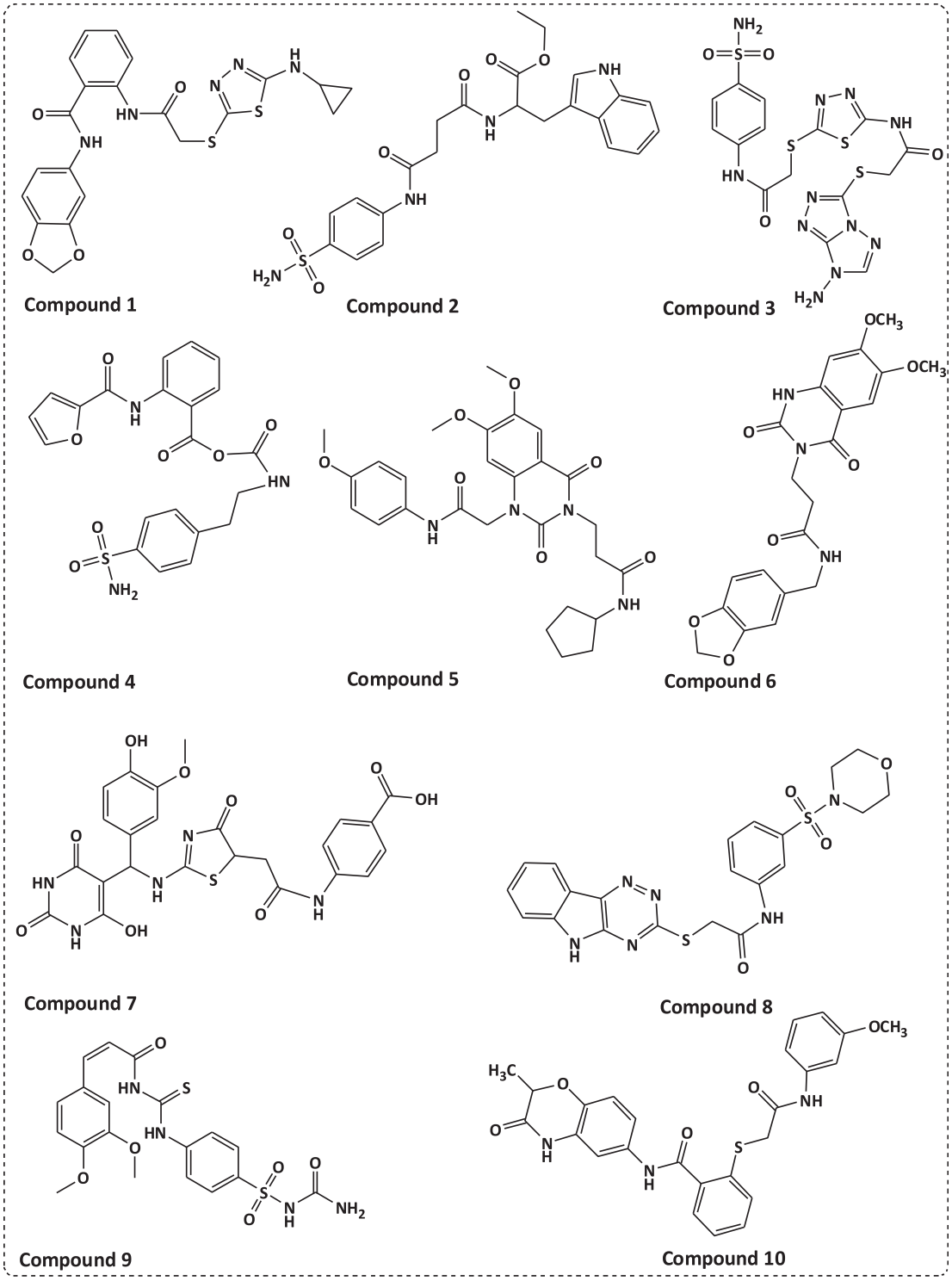

Fig. 1. Chemical structures of potential anti-protease compounds.

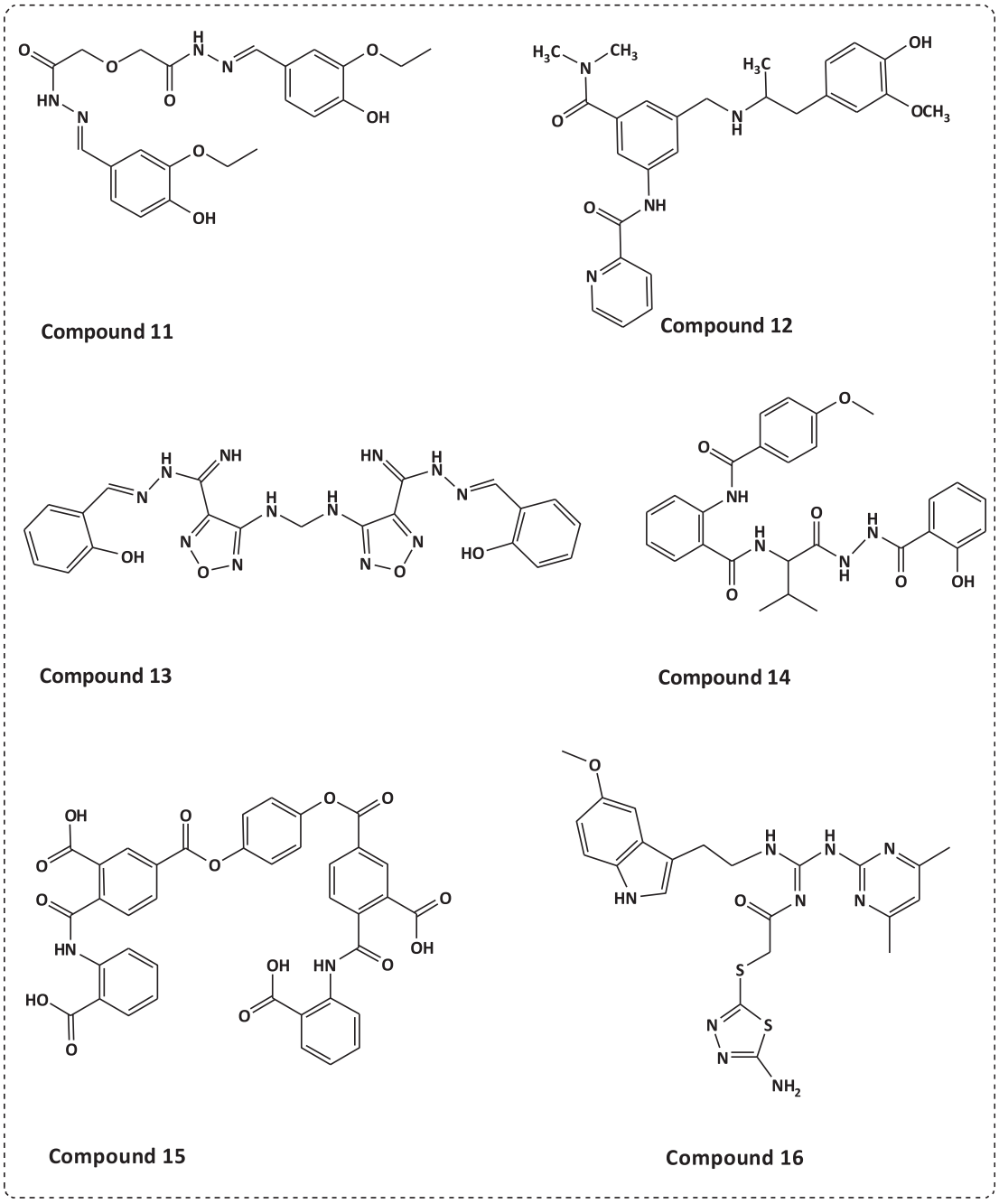

Fig. 1. (*continued*).

passed the PAINS filter were purchased from MCULE and MolPort companies for further biological activities.

The 16 compounds selected with potential binding activity to SARS-CoV-2 M^{pro} following virtual screening were screened against SARS-CoV-2 M^{pro} enzyme compared to positive control (Fig. 4A and Suppl. Table 2). Only compound **13** showed potent inhibition activity (69.8% ± 3.29, $P < 0.0001$) against M^{pro} enzyme, while compound **7** and compound **1** showed partial inhibition activity with inhibition percentage 31 ± 2 and 26.44 ± 1.9, respectively (Fig. 4A). Following the primary screening, compounds **7** and **13** were further tested in dose–response curve. The data showed that IC_{50} of compounds **7** and **13** were 0.45 and 0.11 μM, respectively (Fig. 4B and C). These results indicated that both compounds particularly **13** were more potent against SARS-CoV-2 M^{pro}.

The inhibition activity of the 16 compounds was further tested against SARS-CoV-2 PLpro (Fig. 4D and Suppl. Table 2). Interestingly, compound **13** showed 80%±4 ($P < 0.0001$) inhibition activity, while compound **7** exerted 56.4%±0.3 ($P < 0.0001$) inhibition activity (Fig. 4D). Compound **1**, **2**, **8**, **9** and **12** showed lower inhibition activity of not more than 40% (Fig. 4D). On the other hand, despite the reported anti-HIV activity of compound **14**,[18] it showed no activity against any of SARS-CoV-2 proteases. To calculate the IC_{50} of both compounds **7** and **13**, a dose–response curve was performed. The IC_{50} of compounds **7** and **13** were 0.085 and 0.063 μM, respectively (Fig. 4E and F).

Compounds **7** and **13** were further evaluated against furin protease (Fig. 5A). The data indicated that compounds **7** and **13** showed potential inhibition activity against the enzyme with IC_{50} 0.29 μM (Fig. 5B and C).

These data indicated that compounds **7** and **13** (Fig. 6) showed promising dual inhibition activity against SARS-CoV-2. Compound **13** targeted both viral M^{pro} and PLpro, while compound **7** selectively

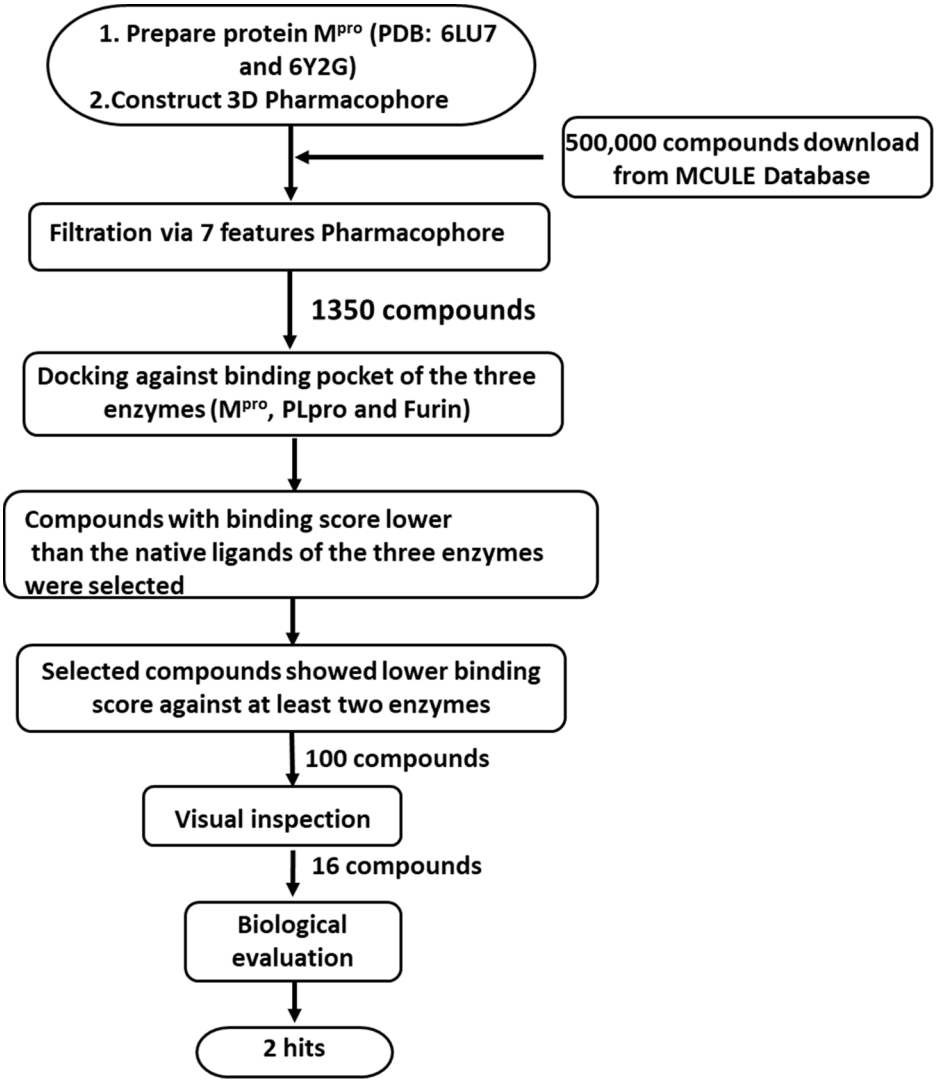

Fig. 2. Schematic representation of pharmacophore structure-based virtual screening.

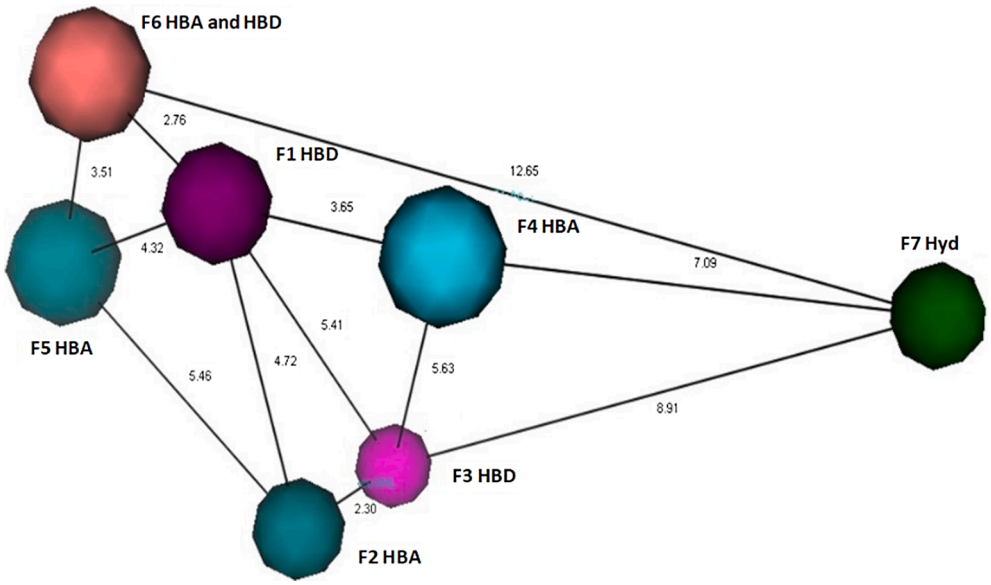

Fig. 3. 3D pharmacophore of the Main protease-ligands interactions. Two hydrogen bonds donor F1, F3 (purple), Three hydrogen bond acceptors F2, F4, F5 (green), one hydrogen bond donor/acceptor F6 (orange) and one hydrophobic interaction F7 (dark green). The numbers represented the distance between the pharmacophore features.

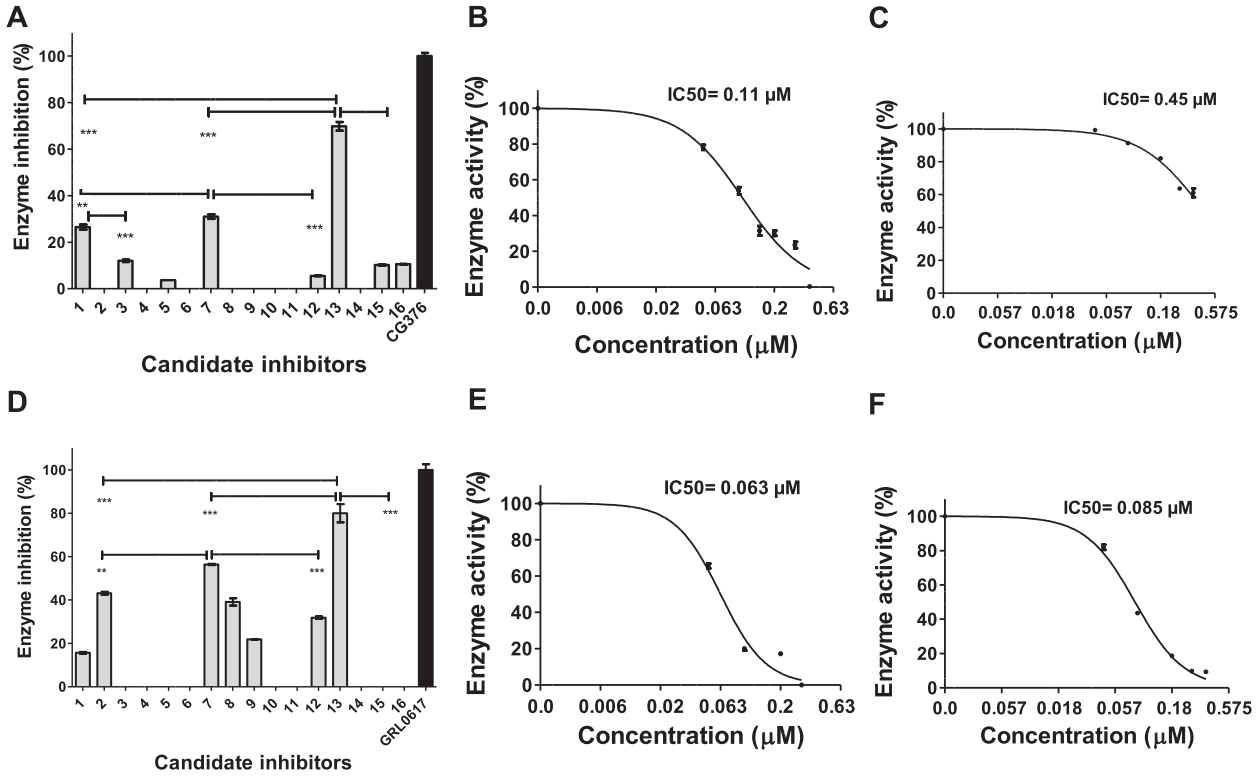

Fig. 4. Inhibition activity of candidate compounds against SARS-CoV-2 proteases. (A) Screening the inhibition activity of the 16 candidate compounds against SARS-CoV-2 M^{pro} at 100 μg/mL. (B) IC_{50} calculation of compound 13 against SARS-CoV-2 M^{pro}. (C) IC_{50} calculation of compound 7 against SARS-CoV-2 M^{pro}. (D) Screening the inhibition activity of the 16 candidate compounds against SARS-CoV-2 PLpro. (D) IC_{50} calculation of compound 13 against SARS-CoV-2 PLpro. (E) IC_{50} calculation of compound 7 against SARS-CoV-2 PLpro. The data was analyzed using one-way ANOVA and statistical significance was calculated with Bonferroni's multiple comparisons test and significance level indicated by asterisks (*, $P < 0.05$; **, $P < 0.01$: ***, $P < 0.001$; ****, $P < 0.0001$). The data display the mean of the percentage of the enzyme inhibition ± SEM of 3 replicas.

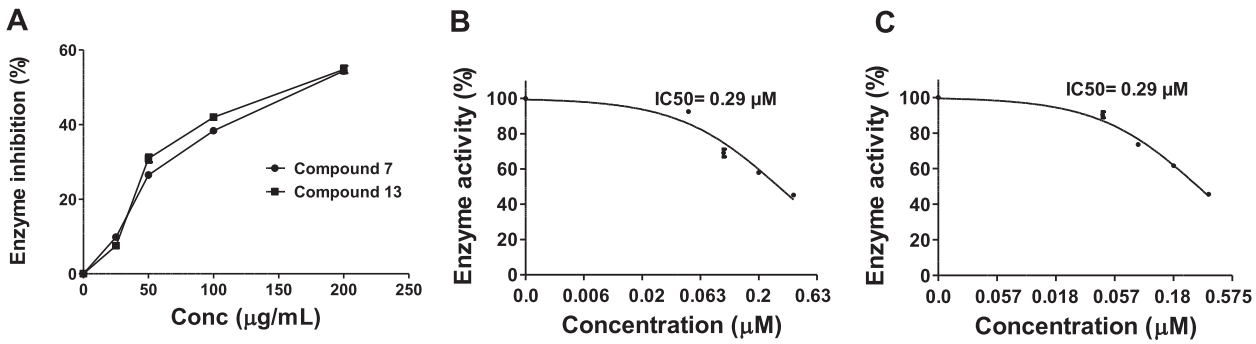

Fig. 5. Inhibition activity of compounds 7 and 13 against human furin protease. (A) Inhibition activity of compounds on furin protease. (B) IC_{50} calculation of compound 13 against human furin protease. (C) IC_{50} calculation of compound 7 against human furin protease. The data display the mean of the percentage of the enzyme inhibition ± SEM of 3 replicas.

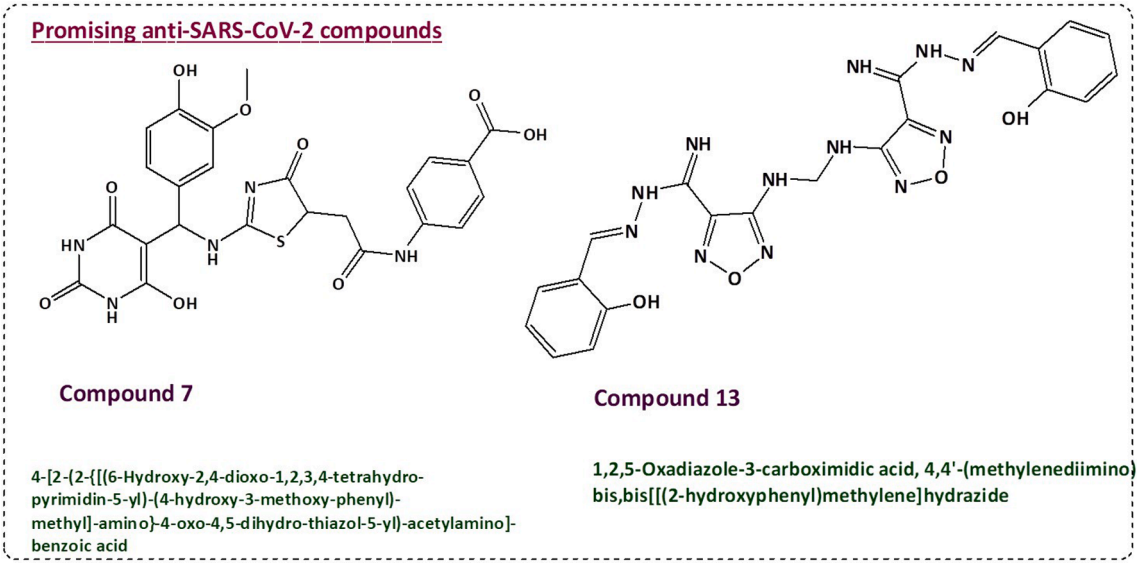

Fig. 6. Chemical structures and names of compounds 7 and 13.

targeted viral PLpro and both compounds showed promising inhibition activity against furin protease. The data obtained constitute solid and promising results toward further confirmation by molecular docking, in vitro and in vivo analysis of both compounds.

The interactions and binding modes of compounds **7** and **13** with SARS-CoV-2 M^{pro}, and PLpro and furin protease were investigated. The results of molecular docking of **7** and **13** were summarized in Table 2. The docking study against M^{pro} revealed that compounds **7** and **13** formed H-bonds with Asn142, while compound **7** formed H-bonds with Thr24, Thr25, and Gln189 (Fig. 7A and Suppl. Fig. 1A). Compound **13** formed H-bond with the key residue Glu166, and π-π interaction with His41 (Fig. 7B and Suppl. Fig. 1B). Both compounds showed hydrophobic interactions with Met49 and Ile141.

Compounds **7** and **13** showed good interaction within PLpro binding site. Both compounds formed H-bond with Lys157 and π-π interaction with Pro284 and Tyr264 (Fig. 7C, D, and Suppl. Fig. 1C, D). Furthermore, compounds **7** and **13** formed H-bonds with His364 and Thr365 of furin protease, while compounds **13** showed additional two H-bonds with Asn295 and Thr368 (Fig. 8A, B, and Suppl. Fig. 1E, F).

We can conclude that compounds **7** and **13** showed strong H-bonds profile and hydrophobic interactions with the three enzymes; however, compounds **13** showed better binding modes than compound **7** and this may explain the potential higher activity of compound **13**.

The in vitro anti-SARS-CoV-2 activity of compounds **7** and **13** was measured against NRC-03-nhCoV, SARS-CoV-2 strain isolated in Egypt, according to Mostafa et al, 2020.[7] The antiviral activity was performed by incubating the compounds at different concentrations with co-cultured viral and Vero-E6 cells. Both compounds **7** and **13** showed significant inhibition activity against SARS-CoV-2 at IC_{50} values of 0.77 and 0.11 μM, respectively (Fig. 9A and B).

The cytotoxic activity of compounds **7** and **13** was performed on normal human fibroblast cells (HDF) using MTT assay. A 50% growth inhibition (IC_{50}) value of both compounds was calculated from dose-response curves obtained from three independent experiments (Fig. 10A and B). Compound **13** showed limited toxicity with IC_{50} 0.41 μM, while compound **7** showed no toxicity and with IC_{50} 1.67 μM.

The results obtained indicated the safety of both compounds, while showing promising antiviral activity against SARS-CoV-2.

The current pandemic caused by the newly emerging coronavirus, SARS-CoV-2, and designated as COVID-19 by WHO poses a serious

Table 2
Molecular modelling study of compounds 7 and 13 within the binding active site of SARS-CoV-2 M^{pro}, PLpro proteases and human furin protease.

Cp	Interacting moiety in the compound	Amino acid involved	Distance Å	Type of interaction
M^{pro}				
7	C═O	OH-Thr24	3.2	H-bond
		OH-Thr25	3.1	H-bond
	NH	C═O Gln189	2.6	H-bond
	OH	C═O Gln189	3.2	H-bond
	C═O	NH Asn142	2.7	H-bond
		Hydrophobic interaction with Met49, Ile141		
13	NH	C═O Glu166	2.7	H-bond
		C═O Glu166	3.0	H-bond
		N-Asn142	2.6	H-bond
	Phenyl ring	π-π interaction with phenyl-His41		
		Hydrophobic interaction with Met49, Phe140, Ile141		
PLpro				
7	C═O	NH Lys157	2.8	H-bond
	Phenyl ring	π-π interaction with Pro248		
	Thiazole	π-π interaction with Tyr264, Tyr268		
13	C═O	NH Lys157	3.1	H-bond
	NH	C═O Glu167	2.8	H-bond
	Phenyl ring	π-π interaction with Pro248		
	Oxadiazole	π-π interaction with Tyr264		
Furin protease				
7	NH	NH Trp254	3.1	H-bond
	C═O	NH His 364	2.8	H-bond
		NHThr365	3.2	H-bond
	Thiazole	π-π interaction with His194		
13	NH	NH Asn295	2.6	H-bond
	O	OH Thr365	2.2	H-bond
	OH	N His364	3.2	H-bond
		NH Thr365	2.9	H-bond
	N	OH Thr368	2.6	H-bond
	Oxadiazole	π-π interaction with His194		

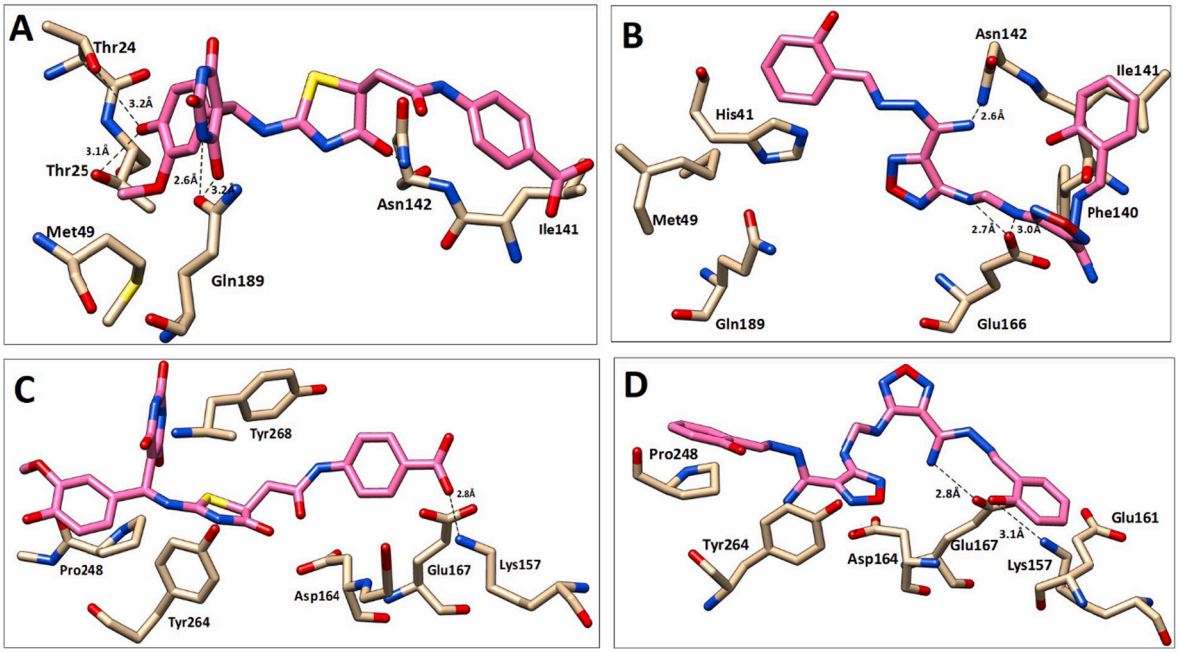

Fig. 7. The interactions of compound 7 and 13 (pink stick) with M^{pro} (PDB: 6Y2G) and PLpro (PDB: 7JRN). The residues of M^{pro} represented as tan stick, and hydrogen bonds are shown as dotted lines. (A) The interaction of compound 7 with M^{pro}. (B) The interaction of compound 13 with M^{pro}. (C) The interactions of compound 7 with PLpro. (D) The interactions of compound 13 with PLpro.

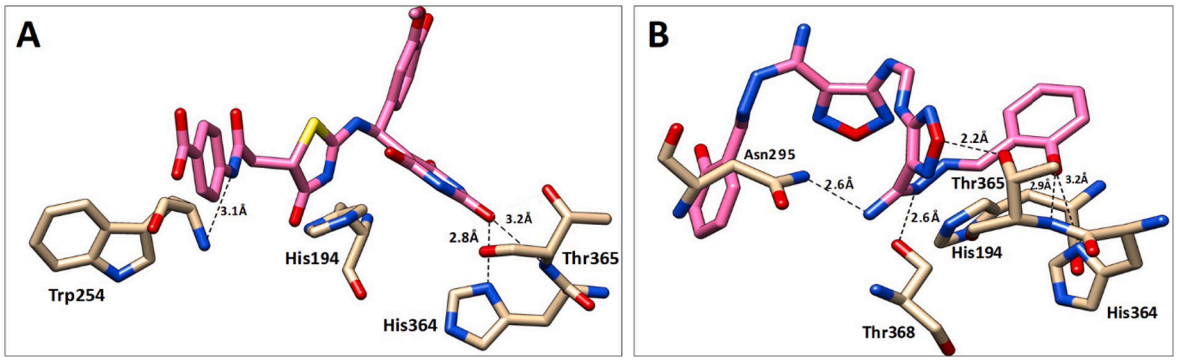

Fig. 8. The interactions of (A) Compound 7 (pink stick) and (B) Compound 13 (pink stick) with furin protease (PDB: 6HLB). The residues represented as tan stick, and hydrogen bonds are shown as dotted lines.

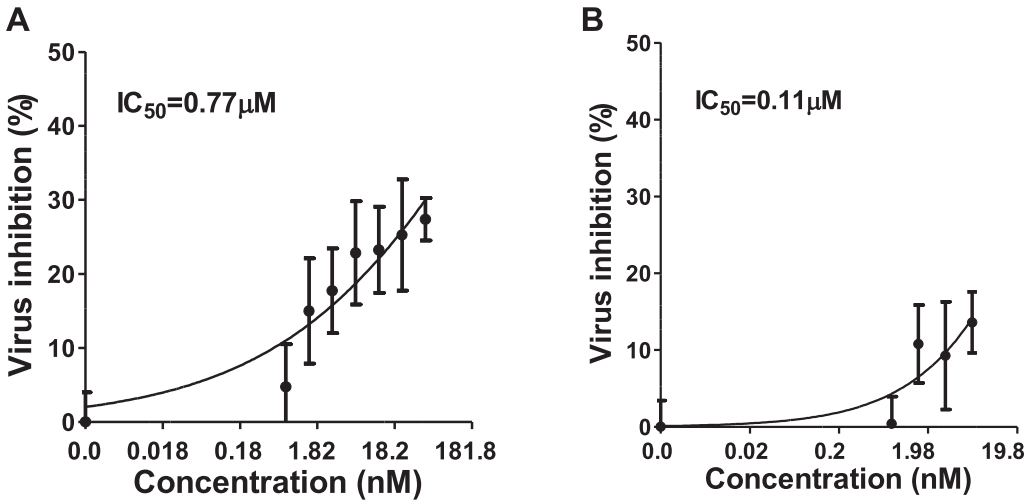

Fig. 9. In vitro antiviral activity of compounds 7 and 13. (A) IC_{50} calculation of compound 7. (B) IC_{50} calculation of compound 13. Inhibitory concentration 50% (IC_{50}) values were calculated using nonlinear regression analysis by plotting log inhibitor concentration versus normalized response (variable slope). The data display the mean of cell viability percentage ± SEM of 4 replicas.

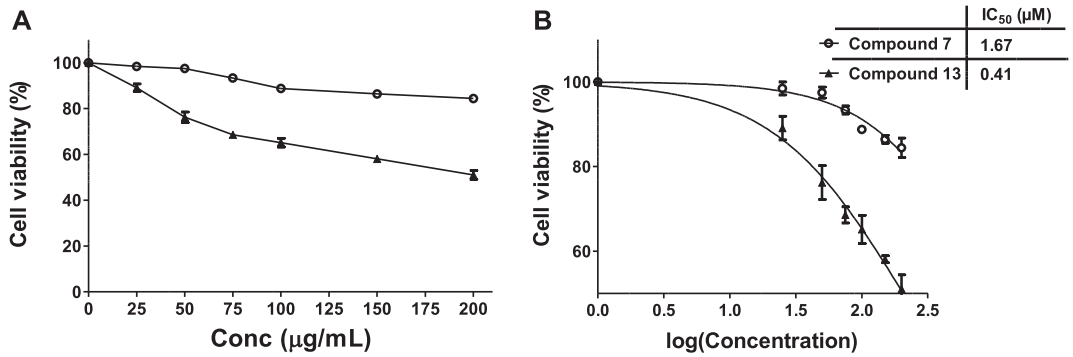

Fig. 10. Cytotoxic activities of compounds 7 and 13. (A) Inhibition activity of compounds 7 and 13 on mammalian cells. (B) IC_{50} calculation of compound 7 and 13 against normal human mammalian cells. The data display the mean of cell viability percentage ± SEM of 3 replicas.

threat to global public health and economy. The newly emerging virus acquired unique structural features that reflect its special pathogenesis and make it difficult to manage. The pathogenesis due to SARS-CoV-2 and the shortage of antiviral drugs challenged all scientists to find effective antiviral drugs either by drug repurposing or discovery of novel drugs. Both viral and human proteins are necessary for the viral activation and infection. SARS-CoV-2 proteases including PLpro, and M^{pro} are well-validated drug targets.[19] PLpro recognizes the C-terminal sequence of ubiquitin, and hence inhibits the host-cell deubiquitinases.[20] M^{pro} proteolytically cleaves the overlapping pp1a and pp1ab polyproteins to functional proteins, which is critical for viral replication.[21] SARS-CoV-2 M^{pro} shows limited mutation rate when compared to SARS-CoV M^{pro} (~96% homology).[22] Both PLpro and M^{pro} showed no genetics homology with the human genome, making them attractive targets for the development of safer antiviral drugs.[23] On the other hand, viral fusion to cell membrane is mediated by the cleavage at S1/S2 site of the S protein following the action of furin protease.[24] This furin-like cleavage site, which is absent in other betacoronaviruses, is

Table 3
Summarized inhibition activities and IC_{50} values of compounds 7 and 13.

Compound	IC_{50} (μM) against				
	M^{pro}	PLpro	Furin	SARS-CoV-2 virus	Mammalian cells (Toxicity)
7	0.45	0.085	0.29	0.77	1.67
13	0.11	0.063	0.29	0.11	0.41

responsible for the high infection and spread rates of the virus.[25] In response, we aimed to bioprospecting novel anti-SARS-CoV-2 drugs with dual action against the viral and host proteases. The purpose for that was not only to target the viral proteins with the lowest mutation rate (M^{pro} and PLpro), but also to overcome any future expected mutation by targeting the human protease (furin). Two compounds **7** and **13**, filtered out of 500,000 compounds, were discovered with promising activity against SARS-CoV-2 by targeting both the viral M^{pro} or PLpro and human furin proteases, while providing safe profile on human cells (summarized in Table 3).

The peptidomimetic-like approach employed in this study by designing drug-like small molecules including compounds **7** and **13** to mimic the peptides, Michael acceptor (peptidyl) inhibitor N3 and α-ketoamide inhibitor 13b, is always used to advantageously improve the stability and biological activity of existing peptides. Further, repurposing marketed drugs is another approach used as fast response to overcome emerging health problem.[26] Interestingly, lopinavir and ritonavir, U.S. FDA-approved viral protease inhibitors,[27] failed in the clinical trial as anti-SARS-CoV-2 inhibitors.[28] Therefore, discovery of novel peptidomimetics drugs with multiple targeting activities is superior.

The overall structure differences of compounds **7** and **13** when compared to the reported M^{pro} protease inhibitors showed unique pharmacophoric features including conformational flexibility and spatial orientation within the binding sites of the targeted proteases. Although the structure of compound **7** is similar to the non-covalent, non-peptide M^{pro} inhibitor that was reported by Zhang et al., 2021,[28] compound **7** showed moderate activity against M^{pro}, but significant inhibition activity against PLpro. The structure differences between both compounds played important role in the fitting of the compound within either M^{pro} or PLpro enzymes. Accordingly, future optimization of compound **7** using free energy perturbation (FEP)-guided design would lead to novel inhibitors with improved efficacy.

In conclusion, the multi-targeting activity, selectivity and promising in vitro inhibition activity of the discovered compounds from this study make them excellent lead compounds for developing more potent anti-SARS-CoV-2 following structure optimization, hybrid synthesis and clinical-based study.

Declaration of Competing Interest

The authors declare that they have no known competing financial interests or personal relationships that could have appeared to influence the work reported in this paper.

Acknowledgement

SA thanks the Advanced Computing Research Centre at the University of Bristol for allowing her to access High -performance Computing.

Funding

The authors acknowledge the generous funding from Sandooq Al-Watan and University of Sharjah to SS under grant #133006.

Appendix A. Supplementary data

Supplementary data to this article can be found online at https://doi.org/10.1016/j.bmcl.2021.128099.

References

1 Huang C, Wang Y, Li X, et al. Novel coronavirus in Wuhan, China. *Lancet*. 2019;395 (2020):497–506.
2 J. Zhang, L. Zhou, Y. Yang, W. Peng, W. Wang, X. Chen, Therapeutic and triage strategies for 2019 novel coronavirus disease in fever clinics, The Lancet Respiratory Medicine, 8 (2020) e11-e12.
3 G. Li E. De Clercq Therapeutic options for the 2019 novel coronavirus (2019-nCoV) 19 3 2020 149 150.
4 Lu H. Drug treatment options for the 2019-new coronavirus 2019-nCoV. *Biosci Trends*. 2020;14:69–71.
5 Amawi H, Abu Deiab GAI, Aljabali AAA, Dua K, Tambuwala MM. COVID-19 pandemic: an overview of epidemiology, pathogenesis, diagnostics and potential vaccines and therapeutics. *Therapeut Deliv*. 2020;11:245–268.
6 Vankadari N. Arbidol: a potential antiviral drug for the treatment of SARS-CoV-2 by blocking the trimerization of viral spike glycoprotein? *Int J Antimicrob Agents*. 2020; 105998.
7 Mostafa A, Kandeil A, Elshaier YAMM, et al. FDA-approved drugs with potent in vitro antiviral activity against severe acute respiratory syndrome coronavirus 2. *Pharmaceuticals*. 2020;13:443.
8 C.f.D.C.a. Prevention, Coronavirus Disease 2019, CDC, CDC Website 2020.
9 Elmezayen AD, Al-Obaidi A, Şahin AT, Yelekçi K. Drug repurposing for coronavirus (COVID-19): in silico screening of known drugs against coronavirus 3CL hydrolase and protease enzymes. *J Biomol Struct Dyn*. 2020:1–13.
10 Ghosh Arun K, Brindisi Margherita, Shahabi Dana, Chapman Mackenzie E, Mesecar Andrew D. Drug development and medicinal chemistry efforts toward SARS-coronavirus and Covid-19 therapeutics. *ChemMedChem*. 2020;15(11):907–932.
11 Walls AC, Park Y-J, Tortorici MA, Wall A, McGuire AT, Veesler D. Structure, function, and antigenicity of the SARS-CoV-2 spike glycoprotein. *Cell*. 2020.
12 Coutard B, Valle C, de Lamballerie X, Canard B, Seidah N, Decroly E. The spike glycoprotein of the new coronavirus 2019-nCoV contains a furin-like cleavage site absent in CoV of the same clade. *Antiviral Res*. 2020;176, 104742.
13 Henrich S, Cameron A, Bourenkov GP, et al. The crystal structure of the proprotein processing proteinase furin explains its stringent specificity. *Nat Struct Mol Biol*. 2003;10:520–526.
14 de Greef JC, Slütter B, Anderson ME, et al. Protective role for the N-terminal domain of α-dystroglycan in Influenza A virus proliferation. *Proc Natl Acad Sci*. 2019;116: 11396–11401.
15 Zhang L, Lin D, Sun X, et al. Crystal structure of SARS-CoV-2 main protease provides a basis for design of improved α-ketoamide inhibitors. *Science*. 2020;368:409–412.
16 Frecer V, Miertus S. Antiviral agents against COVID-19: structure-based design of specific peptidomimetic inhibitors of SARS-CoV-2 main protease. *RSC Adv*. 2020;10: 40244–40263.
17 Shi X, Cheng Q, Hou T, et al. Genetically engineered cell-derived nanoparticles for targeted breast cancer immunotherapy. *Mol Ther*. 2020;28:536–547.
18 Deng J, Sanchez T, Al-Mawsawi LQ, et al. Discovery of structurally diverse HIV-1 integrase inhibitors based on a chalcone pharmacophore. *Bioorg Med Chem*. 2007;15: 4985–5002.
19 Agbowuro AA, Huston WM, Gamble AB, Tyndall JDA. Proteases and protease inhibitors in infectious diseases. *Med Res Rev*. 2018;38:1295–1331.
20 Wu C, Liu Y, Yang Y, et al. Analysis of therapeutic targets for SARS-CoV-2 and discovery of potential drugs by computational methods. *Acta Pharmaceutica Sinica B*. 2020;10:766–788.
21 Hegyi A, Ziebuhr J. Conservation of substrate specificities among coronavirus main proteases. *J Gen Virol*. 2002;83:595–599.
22 Ullrich Sven, Nitsche Christoph. The SARS-CoV-2 main protease as drug target. *Bioorg Med Chem Lett*. 2020;30(17):127377. https://doi.org/10.1016/j.bmcl.2020.127377.
23 Abd El-Mordy FM, El-Hamouly MM, Ibrahim MT, et al. Inhibition of SARS-CoV-2 main protease by phenolic compounds from Manilkara hexandra (Roxb.) Dubard assisted by metabolite profiling and in silico virtual screening. *RSC Adv*. 2020;10: 32148–32155.
24 Xia S, Lan Q, Su S, et al. The role of furin cleavage site in SARS-CoV-2 spike protein-mediated membrane fusion in the presence or absence of trypsin. *Signal Transd Targeted Therapy*. 2020;5:92.
25 Wang J, Ge Y, Xie X-Q. Development and testing of druglike screening libraries. *J Chem Inf Model*. 2018;59:53–65.
26 Cvetkovic RS, Goa KL. Lopinavir/ritonavir. *Drugs*. 2003;63:769–802.
27 Cao B, Wang Y, Wen D, et al. A trial of lopinavir-ritonavir in adults hospitalized with severe covid-19. *N Engl J Med*. 2020;382:1787–1799.
28 Zhang Chun-Hui, Stone Elizabeth A, Deshmukh Maya, et al. Potent Noncovalent inhibitors of the main protease of SARS-CoV-2 from molecular sculpting of the drug perampanel guided by free energy perturbation calculations. *ACS Central Sci*. 2021;7 (3):467–475.